Title
REAL SPACE IMAGE SIMULATION IN HIGH RESOLUTION MICROSCOPY

Authors
Kilaas, R.
Gronsky, R.

Publication Date
1983-03-01

LBL-15345 Rev.
Preprint

Lawrence Berkeley Laboratory
UNIVERSITY OF CALIFORNIA

Materials & Molecular Research Division

Submitted to Ultramicroscopy

REAL SPACE IMAGE SIMULATION IN HIGH RESOLUTION MICROSCOPY

R. Kilaas and R. Gronsky

March 1983

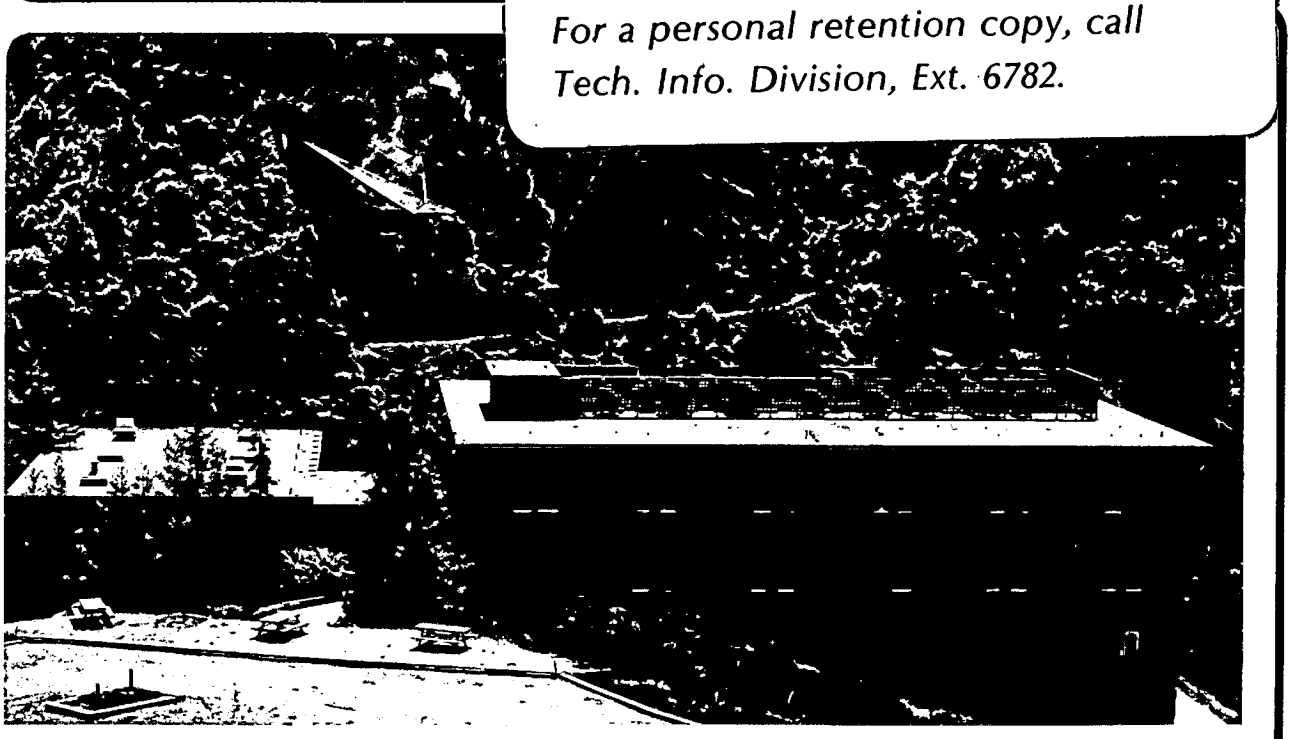

Prepared for the U.S. Department of Energy under Contract DE-AC03-76SF00098

DISCLAIMER

Real Space Image Simulation in High Resolution Microscopy*

R. Kilaas and R. Gronsky

National Center for Electron Microscopy
Materials and Molecular Research Division
University of California
Lawrence Berkeley Laboratory
Berkeley, CA 94720

December 1982
(REVISED: March 1983)

*This work was supported by the Director, Office of Energy Research, Office of Basic Energy Sciences, Materials Sciences Division of the U.S. Department of Energy under Contract No. DE-AC03-76SF00098.

Real Space Image Simulation in High Resolution Electron Microscopy

R. Kilaas and R. Gronsky

National Center for Electron Microscopy
Materials and Molecular Research Division
University of California
Lawrence Berkeley Laboratory
Berkeley, CA 94720

ABSTRACT

The validity of a new method for simulating high resolution electron microscope images has been critically examined. This method, which has been termed the Real Space method since the entire calculation is performed without any Fourier transforms, offers a considerable reduction in computing time over the conventional multislice approach when identical sampling conditions are employed. However, for the same level of accuracy the Real Space method requires more sampling points and more computing time than the conventional multislice method. These characteristics are illustrated with calculated results using both methods to identify practical limitations.

1. Introduction

The current generation of electron microscopes makes possible the attainment of near-atomic resolution [1] in images of crystals; nevertheless there is still an urgent need for reliable computer simulation of these images in order that they might be correctly interpreted [2]. From a pragmatic point of view the full potential of computer simulation is realized only in an on-site, real-time system which affords immediate comparison between computed and experimental results. This is turn requires the development of more rapid and more accurate algorithms.

Most image calculation programs are based upon a dynamical multislice formulation originally proposed by Cowley and Moodie [3] using physical optics. Quantum mechanical arguments were later provided by Van Dyck [4] and independently by Jap and Glaeser [5]. The original calculation time of these early programs is proportional to N^2, N being the number of dynamical reflections included in the calculation. However, using Fast Fourier transforms, Ishizuka and Uyeda [6] demonstrated that the time becomes proportional to N LogN. More recently, a method derived by Van Dyck [7] promises to further reduce the calculation time such that it is directly proportional to N alone. This method, which treats the interaction between the electron beam and the specimen, will be referred to as the Real Space Method since the entire calculation is done in real space without the use of Fourier transforms.

This paper examines the domain of validity of the Real Space method and presents a comparison between the Real Space method and the conventional multislice method. Specific emphasis is placed on the number of dynamical reflections that must be included, maximum slice thickness and calculation time.

2. Theory

2.1 General theory

The geometry of the problem is outlined in Fig. 1. An electron with wave-vector $\underset{\sim}{k}_0$ is incident upon a thin region described by a potential $U(\underset{\sim}{r})$ and for simplicity the electron is assumed to be traveling in the z-direction. In the actual computation the specimen is represented by a sandwich of successive slices, each slice having a thickness ε.

The electron wave function $\Psi(\underset{\sim}{r})$ is a solution to Schrödingers equation

$$\left[- \frac{h^2}{8\pi^2 m} \nabla^2 - eU(\underset{\sim}{r}) \right] \Psi(\underset{\sim}{r}) = \frac{h^2 k_o^2}{2m} \Psi(\underset{\sim}{r}). \qquad (1)$$

For high energy electrons $eU(\underset{\sim}{r}) << \frac{h^2 k_o^2}{2m}$, therefore the potential U can be considered a perturbation and the total wave function can be written as a modulated wave function of the form

$$\Psi(\underset{\sim}{r}) = \phi\ (\underset{\sim}{r})\ e^{2\pi i \underset{\sim}{k_o} \cdot \underset{\sim}{r}} = \phi\ (\underset{\sim}{r}) e^{2\pi i k_o z}. \qquad (2)$$

By inserting the above expression into equation 1, one has

$$\left[\nabla^2 + 4\pi i k_o \frac{\partial}{\partial z} + \frac{8\pi^2 me}{h^2} U(\underset{\sim}{r}) \right] \phi\ (\underset{\sim}{r}) = 0. \qquad (3)$$

By involving the definition

$$V\ (\underset{\sim}{r}) = \frac{8\pi^2 me}{h^2} U(\underset{\sim}{r}) \qquad (4)$$

equation (3) becomes

$$\left[\nabla^2 + 4\pi i k_o \frac{\partial}{\partial z} + V\ (\underset{\sim}{r}) \right] \phi\ (\underset{\sim}{r}) = 0. \qquad (5)$$

At this point it is customary to ignore the second derivative with respect to z in eq. 5 by making the assumption that $\phi\ (\underset{\sim}{r})$ is a slowly varying function with respect to z, such that

$$\left| \frac{\partial^2 \phi}{\partial z^2} \right| << k_o \left| \frac{\partial \phi}{\partial z} \right|$$

This amounts to ignoring backscattered electrons and a slight change in the electron wavevector as the electron traverses the potential. A more complete discussion has been given by Van Dyck [8].

Ignoring the second order derivative transforms eq. 5 into a first order differential equation in z,

$$\frac{\partial}{\partial z}\,\phi(\underset{\sim}{r}) = \frac{i}{4\pi k_o}\left[\,\nabla_{\perp}^2 + V\,(\underset{\sim}{r})\,\right]\phi\,(\underset{\sim}{r}). \tag{7}$$

Formally the solution to (7) can be written

$$\phi\,(x,y,\varepsilon) = e^{\frac{i}{4\pi k_o}\left[\varepsilon\,\nabla_{\perp}^2 + \int_0^{\varepsilon} V\,(\underset{\sim}{r})dz\right]}\,\phi(x,y,o).$$

Note that $e^{A\Psi}$ is defined through the power series

$$e^{A\Psi} = \sum_{n=o}^{\infty}\,(\frac{A^n}{n!})\,\Psi. \tag{8}$$

Defining $\Delta = \frac{i}{4\pi k_o}\,\nabla_{\perp}^2$ and $V_p = \frac{1}{\varepsilon}\,\frac{i}{4\pi k_o}\int_0^{\varepsilon} V(\underset{\sim}{r})dz$

it follows that

$$\phi\,(x,y,\varepsilon) = e^{\varepsilon[\Delta+\,V_p]}\,\phi\,(x,y,o). \tag{9}$$

2.2 Analytical solutions to (9)

Unfortunately there are no closed analytical solution to (9), requiring the use of various approximate solutions.

i) General Multislice

In the formation of the general multislice method one writes

$$\phi\,(x,y,\varepsilon) = e^{\varepsilon[\Delta+V_p]}\,\phi\,(x,y,o) \approx e^{\varepsilon\Delta}e^{\varepsilon Vp}\,\phi\,(x,y,o). \tag{10}$$

Since Δ and V_p do not commute, (10) is correct to first order in ε, Δ and V_p with a resulting error of the order of $\frac{1}{2!}[\Delta,V_p]\varepsilon^2$ where [ ] denotes commutation. The advantage to using equation (10) is that it becomes possible to write down analytical solutions to the expressions

$$f_1\,(x,y,\varepsilon) = e^{\varepsilon Vp}\,f_1\,(x,y,o) \tag{11}$$

$$f_2\ (x,y,\varepsilon) = e^{\varepsilon\Delta}\ f_2\ (x,y,o) \tag{12}$$

of the form

$$f_1\ (x,y,\varepsilon) = \exp\ \{\frac{i}{4\pi k_o} \int_0^{\varepsilon} V\ (x,y,z')dz'\}f_1\ (x,y,o) \tag{13}$$

$$f_2\ (x,y,\varepsilon) = \frac{k_o}{i\varepsilon} \iint dx'dy' f_2(x',y',o)\ \exp\ \{\frac{i\pi k_o}{\varepsilon}\ [(x-x')^2 + (y-y')^2]\}. \tag{14}$$

Defining the functions h and g through the expressions

$$f_1\ (\varepsilon) = h \cdot f_1\ (0)$$

$$f_2\ (\varepsilon) = g * f_2\ (0)$$

equation (10) can be written in alternative form:

$$\phi\ (\varepsilon) = g\ *[h.\phi(0)]. \tag{15}$$

Since the specimen possesses a periodic potential of period ε in the z-direction over its total thickness $N\varepsilon$, it is necessary to use N successive applications of (15). The quickest way to numerically solve the expression

$$\phi\ (N\varepsilon) = g\ *\ [h \cdot [g*[h \cdot [g*[\ .....\ \phi\ (0)]\ ...] \tag{16}$$

is to use Fourier transforms as shown by Ishizuka and Uyeda [6] who utilized the algorithm shown in Fig. 2.

In the remaining part of this paper the general multislice method will be referred to as the FFT method.

ii) Real Space Method

A different approach to finding an approximate solution to (9) is to expand the exponential in powers of Δ and V_p (Van Dyck [7]), and construct a solution that can be written as a product of functions $f_{i,\varepsilon}\ (\Delta)$

$g_{i,\varepsilon}(V_p)$ that when expanded in powers of Δ and V_p corresponds to the expansion of (9) to any desired order of Δ and V_p. A unique solution correct to second order in Δ and V_p was found to be

$$\phi(\varepsilon) = \exp\{\tfrac{1}{2}\varepsilon V_p(1+\delta)\}\exp\{\varepsilon\Delta\}\exp\{\tfrac{1}{2}\varepsilon V_p(1-\delta)\}\phi(o) \quad (17)$$

where

$$\delta \equiv \frac{\bar{z}(x,y)-\varepsilon/2}{\varepsilon/2}, \quad \bar{z} \equiv \frac{\int_o^{\varepsilon} z'V(x,y,z')dz'}{\varepsilon V_p}. \quad (18),(19)$$

The parameter $\delta(x,y)$ is a measure of potential eccentricity and is zero for $\bar{z} = \varepsilon/2$. The major difference between the Real Space (RSP) method and the FFT method is that the RSP method uses an expansion of the propagator, $\exp(\varepsilon\Delta)$, keeping only terms up to second order in ε. The argument is that (17) itself is correct only to second order in ε, and no accuracy should be lost by using an expansion of the propagator. The expression for the propagator thus becomes

$$\exp\{\varepsilon\Delta\} \approx 1+\varepsilon\Delta + \frac{1}{2}\varepsilon^2\Delta^2 = 1 + \frac{i\lambda\varepsilon}{4\pi}\left[\frac{\partial^2}{\partial x^2} + \frac{\partial^2}{\partial y^2}\right]$$

$$- \frac{\lambda^2\varepsilon^2}{32\pi^2}\left[\frac{\partial^2}{\partial x^2} + \frac{\partial^2}{\partial y^2}\right]^2. \quad (20)$$

Numerically one solves the equation

$$f(x,y,\varepsilon) = \exp\{\varepsilon\Delta\}\, f(x,y,o) \approx (1 + \varepsilon\Delta + \frac{1}{2}\varepsilon^2\Delta^2)\, f(x,y,o) \quad (21)$$

by dividing up the x and y axes in intervals of δ and η respectively. Thus

$$f(x,y,\varepsilon) \approx f(x,y,o) + \frac{i\lambda\varepsilon}{4\pi}\{\frac{1}{\delta^2}[f(x+\delta,y,o) + f(x-\delta,y,o) - 2f(x,y,o)]$$

$$+ \frac{1}{\eta^2}[f(x,y+\eta,o) + f(x,y-\eta,o) - 2f(x,y,o)]\}$$

$$- \frac{\lambda^2\varepsilon^2}{32\pi^2}\{\frac{1}{\delta^4}[f(x+2\delta,y,o) + f(x-2\delta,y,o)$$

$$-4f(x+\delta,y,o) - 4f(x-\delta,y,o) - 6f(x,y,o)]\} +$$

$$+\frac{1}{\eta^4}\left[f(x,y+2\eta,o)+f(x,y-2\eta,o)-4f(x,y+\eta,o)\right.$$

$$\left.-4f(x,y-\eta,o)-6f(x,y,o)\right]$$

$$+\frac{2}{\eta^2\delta^2}\left[f(x+\delta,y+\eta,o)+f(x+\delta,y-\eta,o)+f(x-\delta,y+\eta,o)\right.$$

$$\left.+f(x-\delta,y-\eta,o)\right.$$

$$-2f(x+\delta,y,o)-2f(x-\delta,y,o)-2f(x,y+\eta,o)-2f(x,y-\eta,o)$$

$$\left.-4f(x,y,o)\right]. \qquad (22)$$

The computation time for the RSP method becomes proportional to N, the number of sampling points, while it is proportional to NLogN for the FFT method. Another advantage to a real space approach is that it can eliminate the need to use periodic extension when simulating images from faulted crystals.

In the case of a potential having a mirror plane at Z = $\varepsilon/2$, one obtains

$$\phi\,(N\varepsilon) = e^{\frac{1}{2}\varepsilon V_p}\,(1+\varepsilon\Delta+\tfrac{1}{2}\varepsilon^2\Delta^2)e^{\varepsilon V_p}\,(1+\varepsilon\Delta+\tfrac{1}{2}\varepsilon^2\Delta^2)e^{\varepsilon V_p}\,\ldots.$$

$$\ldots.\,(1+\varepsilon\Delta+\tfrac{1}{2}\varepsilon^2\Delta^2)e^{\frac{1}{2}\varepsilon V_p}\,\phi\,(o)\,. \qquad (23)$$

Thus the general multislice calculation becomes accurate to second order for this particular case by simply beginning and ending with half a phase grating.

2.3 The validity of the Real Space Method

Compared to the FFT method, the usefulness of the RSP method depends on the effect of throwing away terms of order (ε^3,Δ^3) in (20). The error depends on the slice thickness ε as well as the magnitude of the derivatives. By studying the effect of the operator exp $\{\varepsilon\Delta\}$ on the function $\phi(x,y,o)$, one notices that in reciprocal space the effect is that of a pure phase-operator.

$$\Phi\ (\underset{\sim}{g}.o) \equiv \iint dxdy\phi(\underset{\sim}{\rho},o)e^{-2\pi i\underset{\sim}{g}\cdot\underset{\sim}{\rho}} \tag{24}$$

$$\Phi\ (\underset{\sim}{g},\varepsilon) \equiv \iint dxdy[e^{\varepsilon\Delta}\phi(\rho,o)]e^{-2\pi i\underset{\sim}{g}\cdot\underset{\sim}{\rho}} = \Phi(\underset{\sim}{g},o)e^{-i\pi\lambda\varepsilon g^2} \tag{25}$$

The expansion of the propagator to second order in ε and Δ is equivalent to writing

$$\Phi\ (\underset{\sim}{g},\varepsilon) \approx (1 - i\pi\lambda\varepsilon g^2 + \tfrac{1}{2}\pi^2\lambda^2\varepsilon^2 g^4)\ \Phi(\underset{\sim}{g},o) \tag{26}$$

such that the intensity of the corresponding reflection after the electron has traveled the distance ε, is

$$I\ (\underset{\sim}{g},\varepsilon) \equiv |\Phi(\underset{\sim}{g},\varepsilon)|^2 = [1 + \tfrac{1}{4}\ (\pi\lambda\varepsilon g^2)^4\ ]\ I\ (\underset{\sim}{g},o). \tag{27}$$

To make sure that high order reflections (large g-vector) are not significantly amplified through the action of the propagator, it is necessary to use a slice thickness ε and an effective g_{max} such that

$$\frac{\pi\lambda\varepsilon}{\sqrt{2}}\ g^2max << 1 \text{ or } \lambda\varepsilon g^2_{max} << \frac{\sqrt{2}}{\pi} = 0.45. \tag{28}$$

For a periodic potential, period a, of cubic symmetry, the only g-vectors allowed are of the type $g_x = \frac{h}{a}$, $g_y = \frac{k}{a}$; h,k integers. For a numerical calculation with N sampling points in the x-and y-direction, δ= a/N and η= a/N. The equivalent expression to (27) is obtained by inserting eq. (22) into the expression

$$\Phi\ (u,v,\varepsilon) = \sum_{x,y}\ \phi\ (x,y,\varepsilon)e^{-2\pi iux-2\pi ivy}$$

and letting u = h/a and v = k/a.

This gives

$$I(h,k,\varepsilon) = I(h,k,o)\cdot\{1 + (\frac{\lambda\varepsilon N^2}{4\pi a^2})^4 [\cos 4\pi h/N + \cos 4\pi k/N - 8\cos 2\pi h/N - 8\cos 2\pi k/N + 2\cos 2\pi(h+k)/N + 2\cos 2\pi(h-k)/N + 10)^2\}. \quad (29)$$

For the special case of h = k,

$$I(h,h,\varepsilon) = I(h,h,o)\cdot\{1 + (\frac{\lambda\varepsilon N^2}{4\pi a^2})^4 [4\cos 4\pi h/N - 16\cos 2\pi h/N + 12]^2\}. \quad (30)$$

By dividing the a-axis up into N intervals, one is limited to $g_{max} = \frac{hmax}{a} = \frac{N}{2a}$. This gives

$$I(h_{max},h_{max},\varepsilon) = I(h_{max},h_{max},o)\cdot\{1 + (\frac{4\sqrt{2}\lambda\varepsilon}{\pi} g_{max}^2)^4\} \quad (31)$$

and correspondingly one must impose

$$\lambda\varepsilon g_{max}^2 << \frac{\pi}{4\sqrt{2}} = 0.56. \quad (32)$$

Equations (28) and (32) set an upper limit on the slice thickness and the number of reflections that can be included in the calculation. The slice thickness ε and the number of sampling points in each direction x and y must be chosen so as to satisfy

$$K_{max} \equiv \lambda\varepsilon g_{max}^2 << \frac{1}{2}. \quad (33)$$

3. Results of Computer Calculations

In order to compare the Real Space method with the conventional multi-slice method using fast Fourier transforms, programs were written that could be run in either FFT or RSP mode. To make it possible to use different values for the slice thickness, a three dimensional potential

was calculated through a 3 dimensional Fourier transform. The specimen is copper (lattice const. 3.6Å) and the c-axis (z-dir.) was divided into 16 intervals such that a slice thickness of either 3.6Å, 1.8Å, 0.9Å or 0.45Å could be used. To be able to compare the results of the two methods under various conditions, amplitudes and phases of selected reflections were plotted as a function of thickness.

Figure 3 shows what happens when $K \equiv \lambda\varepsilon g_{max}^2$ increases beyond the critical value of 1/2. The reflections are 000, 200, 220 and 440 and the solid line is the result of the FFT method while the broken line represents the RSP method. Only amplitude vs. thickness is plotted and the slice thickness is kept constant at 3.6Å. The maximum reciprocal lattice vector g_{max} takes on the values of $1.4Å^{-1}$, $1.9Å^{-1}$ and $2.5Å^{-1}$ to give a value for K of 0.18, 0.33 and 0.57 respectively.

As K increases the discrepancy between the two methods decreases, and significantly, when K increases beyond its critical value the RSP method starts to diverge. For this particular value of K the divergence sets in at about 100Å and the intensity of the reflection 400 is seen to start growing almost exponentially. At about 100Å there is enough intensity in the 440 reflection for it to be affected by the action of the propagator. The low order reflections are not affected directly by the propagator, although they are influenced by the interaction with higher order reflections through the crystal potential.

Figure 4 shows the amplitudes and phases of various reflections for 3 different values of ε and g_{max} keeping K constant at 0.25. Notice that while in Figure 1 the accelerating voltage is 200kV, it is

now set at 1MV. The FFT calculation is almost unaffected by changes in ε and g_{max} (the results for ε= 3.6Å and g_{max} = 2.8Å are shown here) indicating that for $g_{max} > 2.8\text{Å}^{-1}$, no appreciable aliasing effects are introduced. However, the results of the RSP calculation vary significantly as g_{max} increases (ε decreases), but the results of the RSP method approach that of the FFT method as the number of reflections included in the calculation increases.

Figure 5 shows the result of the RSP calculation for three different values of the slice thickness, at constant g_{max} equal to 2.8Å^{-1}. Although the results vary somewhat depending on the slice thickness, reducing the slice thickness does not have a major effect; i.e. it does not cause the result of the RSP method to approach that of the FFT calculation.

Finally, Table 1 shows some computation times for the FFT and RSP methods. The times that are given are the computational times per slice for a slice thickness of 3.6Å at three different numbers of sampling points. Using ε= 3.6Å obviously results in the fastest calculation since it is only necessary to calculate one $V_p(x,y)$. The programs were all run on a CDC 7600 computer.

4. Discussion

The primary motive behind the formulation of the Real Space method as an alternative way to do computer simulation of electron microscope images is that the RSP method appears to offer the following advantages:

1. There is no error due to aliasing which might occur when using Fourier transforms.

2) There is a possibility of eliminating the need to use periodic extension in faulted crystals.

3) The method might allow using a larger slice thickness, being correct to second order in ε.

4) A reduction in computer time is possible for the RSP method, the time per slice being proportional to N, the number of sampling points, rather than NLogN as for the FFT method.

As to the first claim, it is true that there is no aliasing associated with the RSP method. However, when all the physically relevant reflections are taken into account in an FFT calculation, aliasing should not be a problem. Rather one can argue that if aliasing ever does affect the result, not enough reflections have been included to give a meaningful result anyway. Although there has been no attention given here to determining when aliasing begins to affect the FFT calculation, the above results indicate that for an accelerating voltage of 1MV, no such effect occurs as long as $g_{max} > 2.8\mathring{A}^{-1}$.

In most cases it will be possible to avoid using a periodic unit cell in an RSP calculation and thus avoid the need to use a periodic continuation when simulating images of defective crystals. The choice to use periodic continuation or not depends on how one decides to calculate the derivatives at the boundary of the x-y plane.

With respect to the third possible advantage, it is instructive to examine the asymptotic behavior of the RSP method as the slice thickness is decreased and the number of sampling points is increased. The first condition imposed on the RSP method is that $K = \lambda\varepsilon g_{max}^2 << 1/2$. Similarly, a limit on K is also imposed in the conventional multislice method.

For example, Ishizuka and Uyeda [6] using a stationary phase method in deriving the multislice formula arrive at the condition $K \ll 1$. Lynch and O'Keefe [9] argue that to avoid upper layer line reinforcement, the parameter for the pseudo-layer interaction $\alpha(g) = \frac{1}{2}\lambda\varepsilon g^2$ should be less than 0.5. This again corresponds to $K<1$, however for safety, a value of $K_{max} = 0.2$ was used. Thus the major difference between the RSP method and the FFT method in this respect is that while an RSP calculation for $K_{max} > 1/2$ begins to diverge, the corresponding FFT calculation does not. In either case, care should be taken with respect to the size of the slice thickness and the number of reflections needed to satisfy the condition $K < 1/2$.

However, in spite of similar conditions imposed on the two methods, it is seen from the results of the computer calculations that there are important differences between the RSP and FFT methods. Only as the slice thickness decreases and the number of reflections increases, does the result of the RSP calculation approach that of the FFT calculation. Furthermore while the FFT method is barely affected by changes in ε and g_{max} (as long as $\varepsilon \lesssim 3.6\mathring{A}$ and $g_{max} \gtrsim 2.8\mathring{A}^{-1}$ for V_o = 1MV), the RSP calculation is strongly affected. Reducing the slice thickness gives only minor changes in the result of the RSP calculation, which means that the number of reflections included in the calculation has the strongest influence on the result. Although the need to incorporate reflections beyond $2.8\mathring{A}^{-1}$ is not indicated for the FFT approach, this may be necessary in the RSP approach to ensure that none of the relevant reflections become artifically amplified through the action of the expanded propagator. Thus instead of being able to use a larger slice thickness in the RSP method compared to the FFT method, it seems more likely that a smaller slice thickness is essential in order

to accommodate the inclusion of a larger number of reflections.

Finally, under identical conditions the RSP method offers a significant reduction in computer time. For the range of commonly used N (number of sampling points), the reduction in computer time per slice amounts to a factor of 3-5. This represent a significant saving in computer time and could prove to be a great value when using smaller and slower computers. It must however be noted that the saving is in calculation time per slice for the same N and is only effective if the same slice thickness and the same number of reflections can be used in the two methods.

5. Conclusion

The RSP method gives results similar to the conventional multislice calculation when care is taken to include enough reflections. To keep within the domain of validity of the RSP method, it might be necessary to reduce the slice thickness as the number of reflections increases, as needed to maintain $\lambda\varepsilon g_{max}^2 < 1/2$. If this condition is not satisfied, the RSP method will begin to diverge due to a near-exponential growth of higher order reflections. The divergence is due to the amplification effect of the expanded propagator and does not set in until a nominally low intensity has been scattered into those reflections having g-vectors with magnitude close to g_{max}. Although a similar boundary condition is imposed on the validity of the FFT method, going beyond the domain of validity does not cause any divergence. In order to obtain reliable results from the RSP method it might be necessary to include more reflections than required with the FFT method which consequently also requires smaller slice thicknesses and therefore increased computational time. Investigations into further improvements of, and extended applications

of the Real Space method are currently underway.

6. Acknowledgements

The authors gratefully acknowledge helpful suggestions by Drs. D. Van Dyck, M.A. O'Keefe and W.O. Saxton.

This work was supported by the Director, Office of Energy Research, Office of Basic Energy Sciences, Materials Science Division of the U.S. Department of Energy under Contract No. DE-AC03-76SF00098.

7. References

[1] R. Gronsky, in 38th. Ann. Proc. Electron Microscopy Soc. Amer., San Francisco, CA., 1980, G.W. Bailey (ed.), p. 2.

[2] W.O. Saxton, Advances in Electronics and Electron Physics, Suppl. 10, Academic Press Inc., New York, L. Marton (ed.), p. X1.

[3] J. M. Cowley and A. F. Moodie, Acta Cryst. 10, (1957), p. 609.

[4] D. Van Dyck, Acta Cryst. A34, (1978), p. 94.

[5] B. Jap and R. Glaeser, Acta Cryst. A34, (1978), p. 112.

[6] K. Ishizuka and N. Uyeda, Acta Cryst. A33, (1977), p. 740.

[7] D. Van Dyck, Journal of Microscopy, 119, (1980), p. 141.

[8] D. Van Dyck, Phys. Stat. Sol., B72, (1976), p. 321.

[9] D. F. Lynch and M. A. O'Keefe, Acta Cryst. A28, (1972), p. 536.

FIGURE CAPTIONS

Fig. 1. Schematic representation of the scattering problem. The specimen is depicted as a potential distribution U ($\underset{\sim}{r}$) which may be divided into a series of slices having thickness ε.

Fig. 2. Schematic representation of the fast Fourier transform (FFT) algorithm used by Ishizuka and Uyeda [6].

Fig. 3. Amplitude vs. thickness for the reflections 000, 200, 220 and 440 for copper [001]. Accelerating voltage is 200kV and the slice thickness is 3.6Å. The result from the FFT calculation is shown by the solid line, and the broken line represents the RSP calculation. In the first column $g_{max} = 1.4^{\circ -1}$ (K = 0.18), in the second column $g_{max} = 1.9\mathring{A}^{-1}$ (K = 0.33) and in the third column $g_{max} = 2.5\mathring{A}^{-1}$ (K = 0.57).

Fig. 4. Amplitude and phase (in uints of π) vs. thickness for 3 sets of values of the slice thickness ε and g_{max}. The values are (1) $\varepsilon = 3.6\mathring{A}$, $g_{max} = 2.8\mathring{A}^{-1}$; (2) $\varepsilon = 1.8\mathring{A}$, $g_{max} = 3.9\mathring{A}^{-1}$; (3)$\varepsilon = 0.9\mathring{A}$, $g_{max} = 5.5\mathring{A}^{-1}$ labeled separately for the RSP method. These values gave essentially the same results for the FFT method, plotted as the single FFT curve.

Fig. 5. Amplitude and phase (in units of π) vs. thickness for 3 different valuesof the slice thickness ε ; g_{max} is kept constant at $2.8\mathring{A}^{-1}$, ε takes the values 3.6A (-), 1.8A (---) and 0.9A (++). Calculation is by the RSP method.

N_x, N_y	$N_x^N, \bar{N}_y$	t_{RSP} [sec]	t_{FFT} [sec]
20	400	0.017	0.063
28	784	0.034	0.12
40	1600	0.066	0.23

Table 1. Computational times per slice, slice thickness 3.6A, for the FFT method and the RSP method at three different values of the number of sampling points N.

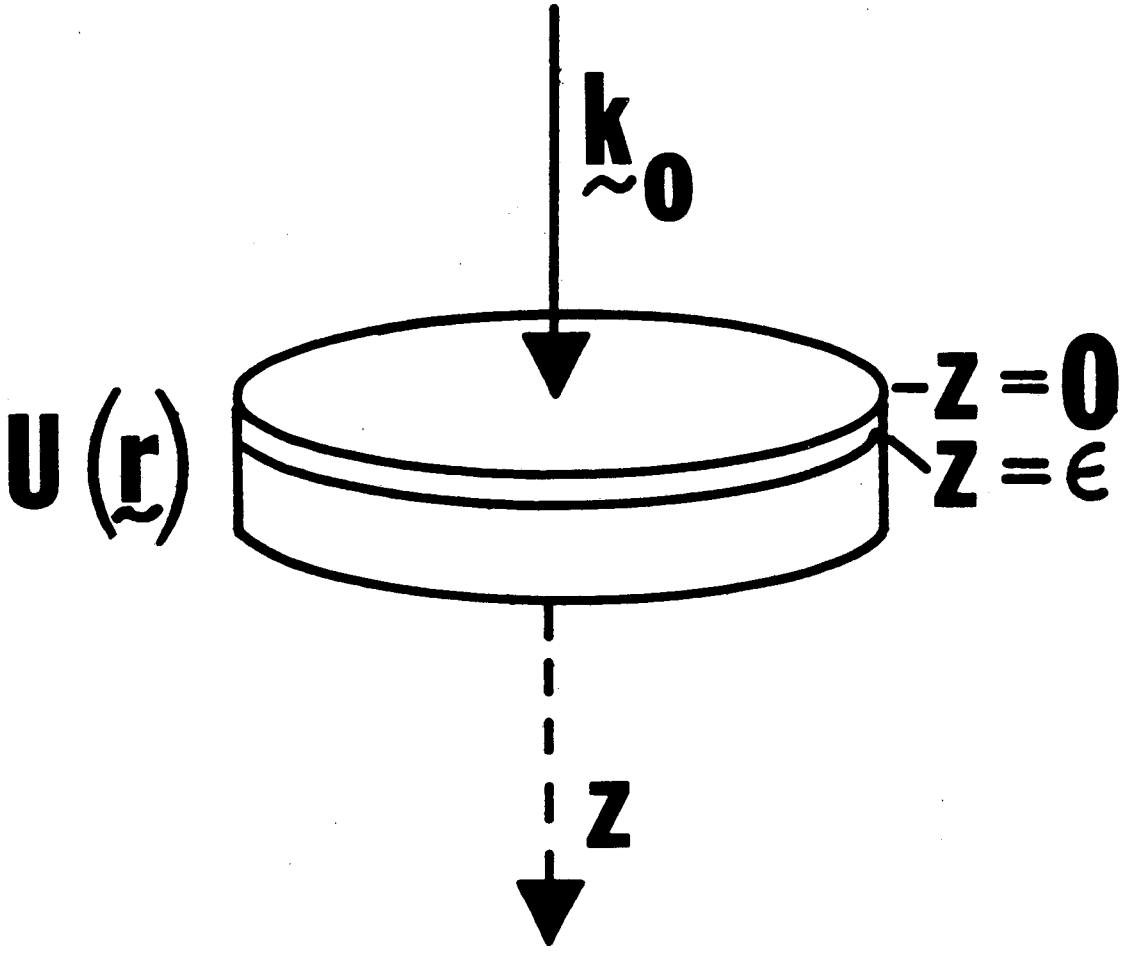

XBL 8212-12231

Fig. 1

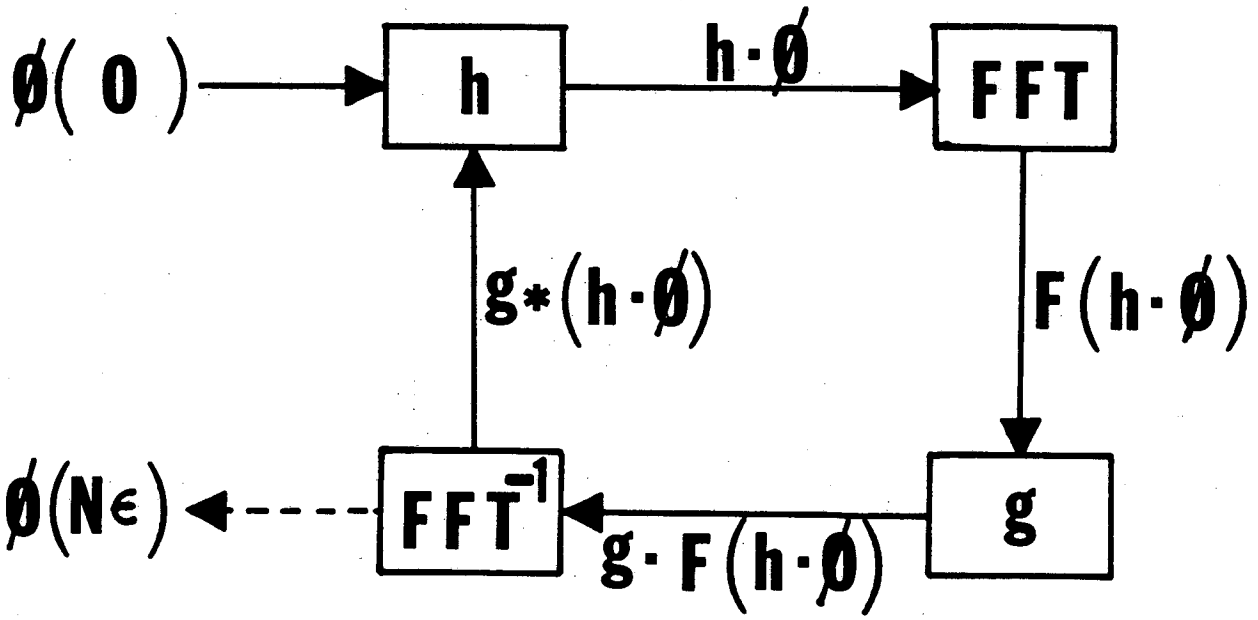

XBL 8212-12232

Fig. 2

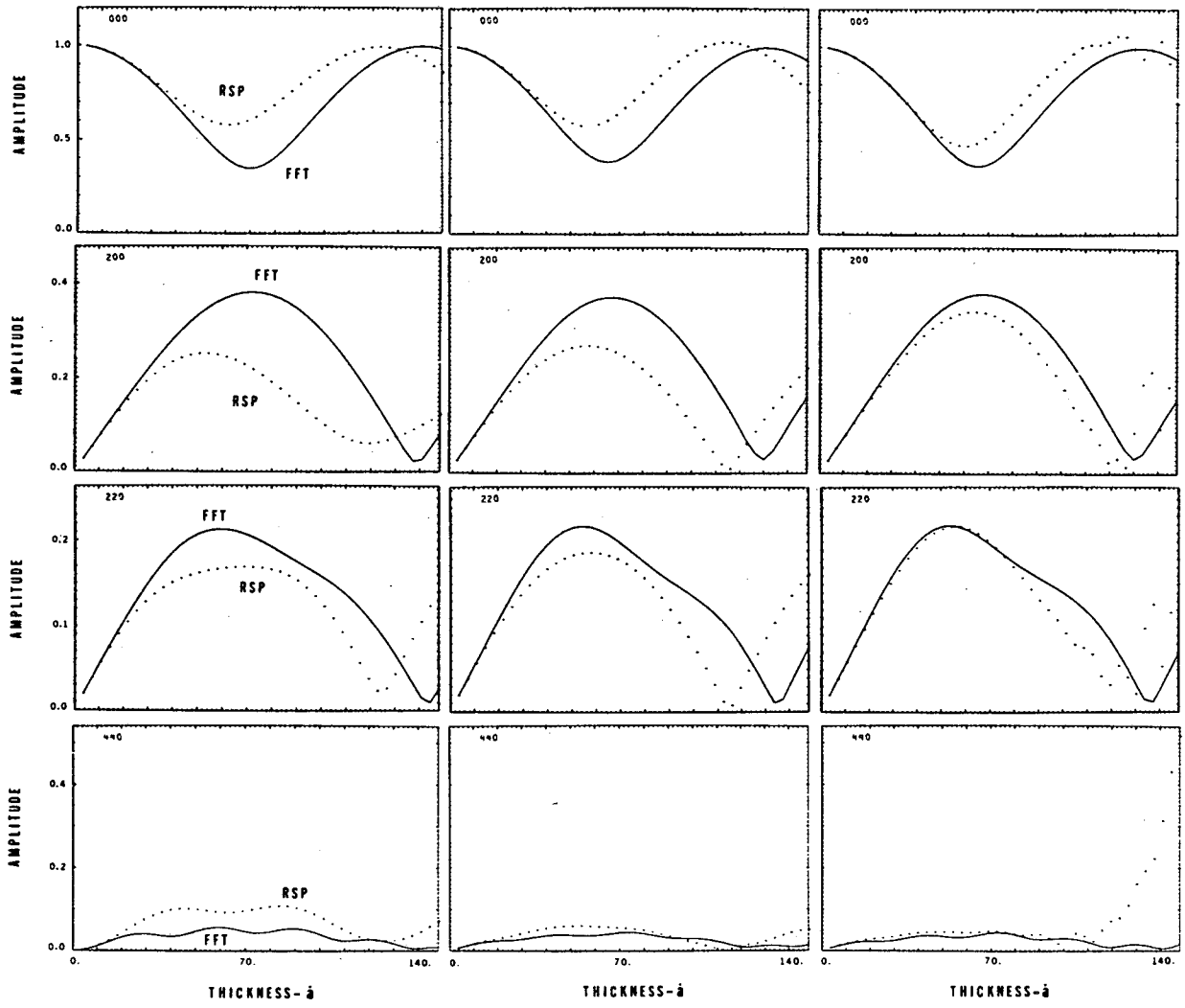
000
200
220
440
RSP
FFT
AMPLITUDE
THICKNESS-Å
0.
70.
140.
GMAX = 1.4Å⁻¹
K = 0.18
GMAX = 1.9Å⁻¹
K = 0.33
GMAX = 2.5Å⁻¹
K = 0.57
VOLTAGE = 200 KV
XBL 833-8924

Fig. 3

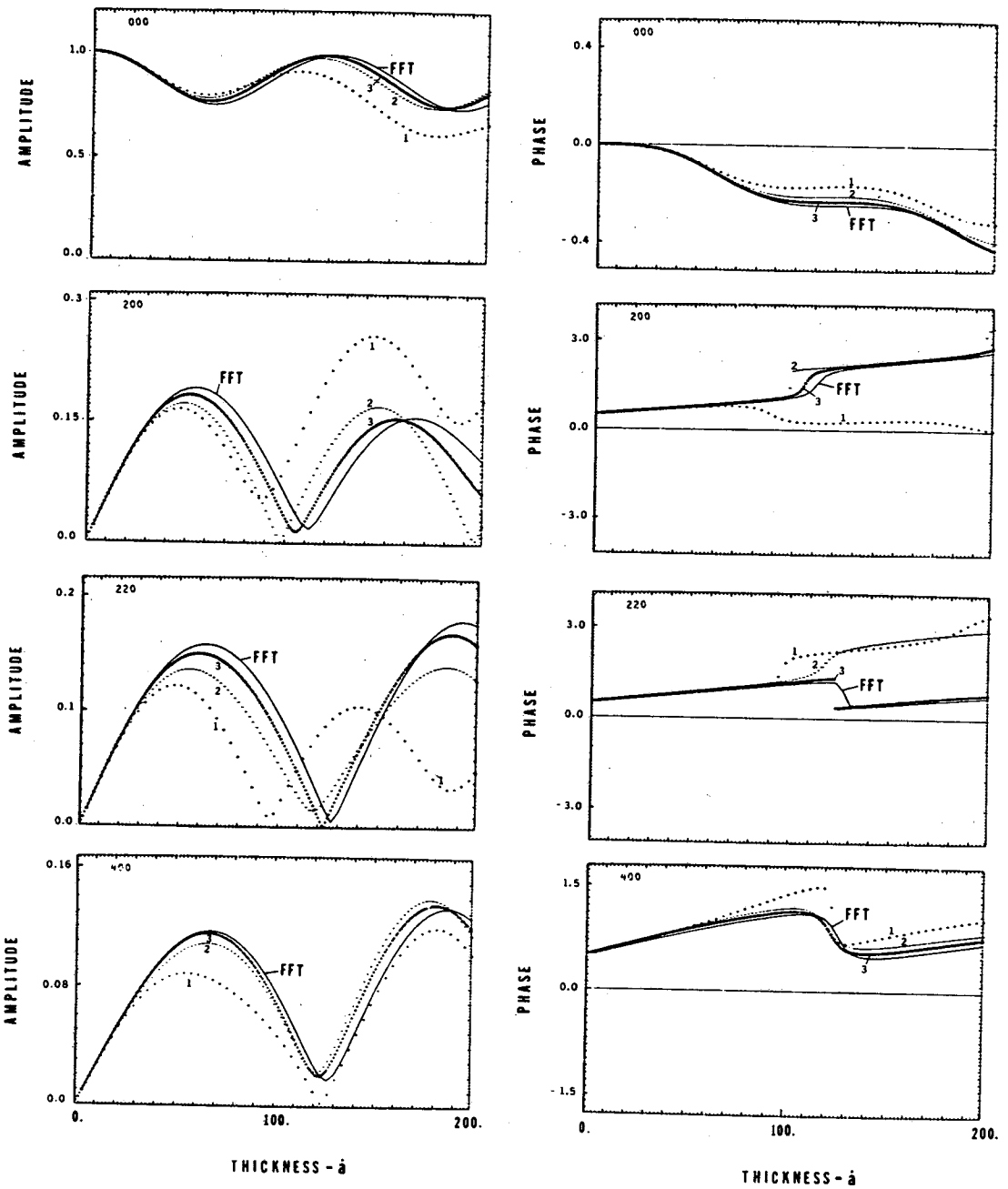

VOLTAGE = 1000 KV

K = 0.25

XBL 833-8922

Fig. 4

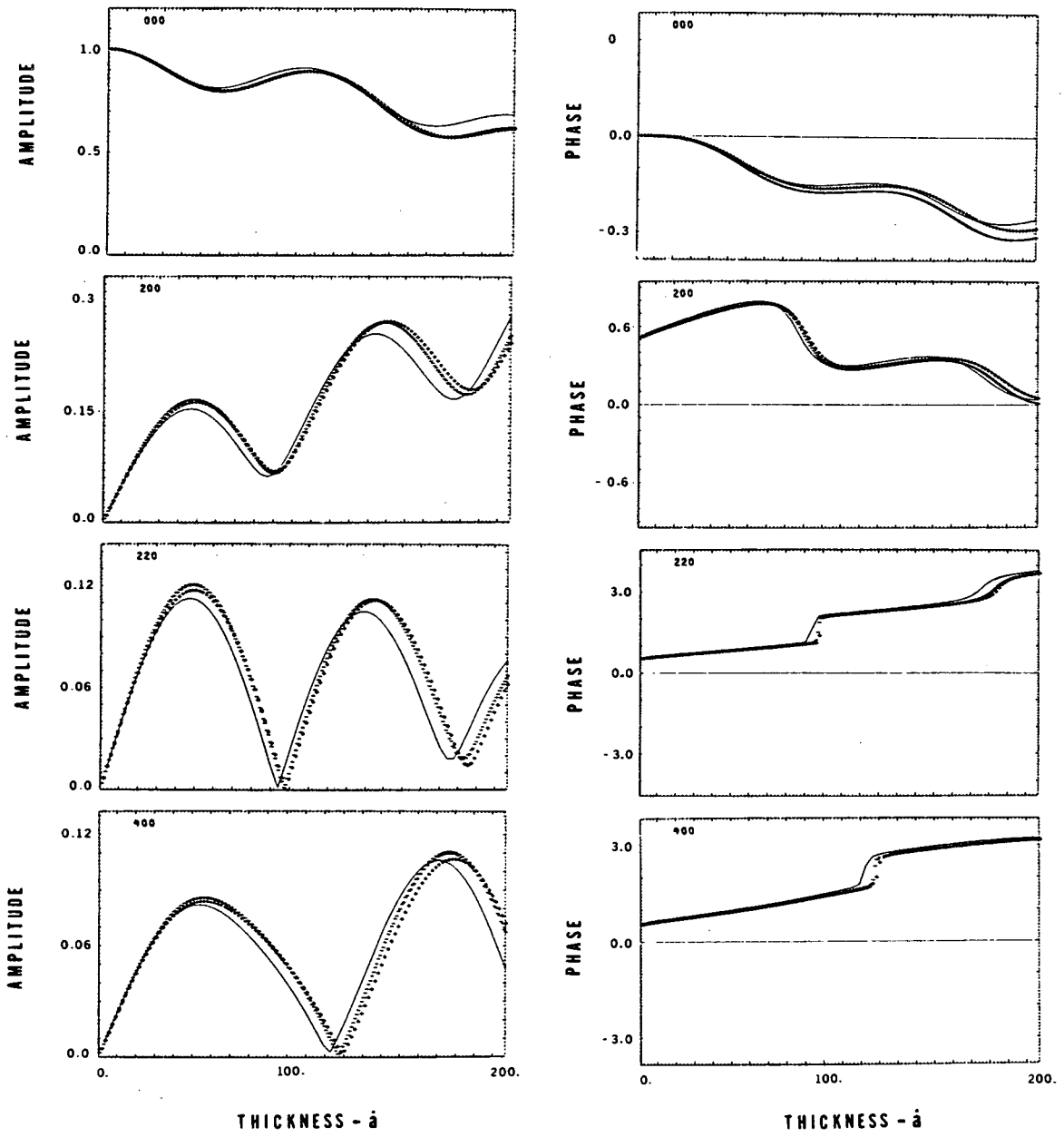
COPPER 001
AMPLITUDE
PHASE
000
200
220
400
1.0
0.5
0.0
0.3
0.15
0.12
0.06
0
-0.3
0.6
-0.6
3.0
-3.0
0.
100.
200.
THICKNESS - å
GMAX = 2.8 å⁻¹
VOLTAGE = 1000 KV
XBL 833-8923

Fig. 5

TECHNICAL INFORMATION DEPARTMENT
LAWRENCE BERKELEY LABORATORY
UNIVERSITY OF CALIFORNIA
BERKELEY, CALIFORNIA 94720